

Correlated conductivity and work function changes in epitaxial graphene

Md. W. K. Nomani,^{1,a)} V. Shields,² G. Tompa,³ N. Sbrockey,³ M. G. Spencer,² R. A. Webb,⁴ and G. Koley¹

¹Department of Electrical Engineering, University of South Carolina, Columbia, South Carolina 29208, USA

²Department of Electrical and Computer Engineering, Cornell University, Ithaca, New York 14853, USA

³Structured Materials Industries, Inc., Piscataway, New Jersey 08854, USA

⁴Department of Physics and Astronomy, University of South Carolina, Columbia, South Carolina 29208, USA

(Received 3 October 2011; accepted 14 February 2012; published online 2 March 2012)

Correlation between conductance and surface work function (SWF) changes caused by molecular adsorption on epitaxial graphene on both faces of 6H-SiC has been investigated. The SWF and conductance changes, explained on the basis of graphene band diagram, indicate C-face multilayer and Si-face few layer graphene behave as p and n-type sensing layers, respectively. A quantitative model correlating conductance and SWF changes has been proposed within the framework of Boltzmann transport theory. Our results further indicate that for epitaxial graphene, the charge interaction by the adsorbed molecules and related work function changes can be strongly influenced by the SiC substrate. © 2012 American Institute of Physics. [<http://dx.doi.org/10.1063/1.3691628>]

Since its invention in 2004, graphene, a two-dimensional (2D) monolayer of sp^2 bonded carbon atoms, has attracted huge interest among researchers, due to its distinctive mechanical, thermal, and electrical properties.^{1–3} In particular, graphene exhibits remarkably high carrier mobility up to $200\,000\text{ cm}^2\text{ V}^{-1}\text{ s}^{-1}$ in suspended form,⁴ as the charge carriers resemble Dirac fermions; and the carrier transport can remain ballistic up to $0.3\text{ }\mu\text{m}$ in ambient conditions.¹ However, due to different sources of scattering, this value is highly reduced in supported graphene.⁵ Due to the atomically thin nature of the graphene films, their electronic and transport properties are readily affected by adsorbed impurities, which can open up applications of these films in a wide range of sensor devices. Indeed, a wide variety of graphene based sensor devices have been reported for sensing toxic gases, chemicals, explosives, and radiation,^{6–8} taking advantage of the unique material properties of graphene.

For successful development of graphene based sensors and electronics, availability of high quality and large area graphene films is necessary, and epitaxial graphene grown on SiC substrates by graphitization has been shown to be quite satisfactory both in terms of quality and reliability.^{9–11} Graphene on SiC substrate offers the added advantage of integrating sensors and readout circuits on the same chip, that are also suitable for harsh environment operation, taking advantage of the wide bandgap of SiC.¹² Although surface work function (SWF) measurements on graphene have been reported by several groups,^{13–15} including preliminary studies of SWF and conductance changes due to molecular adsorption,¹⁶ a direct and quantitative correlation between the Fermi level movement and the corresponding conductance change, caused by adsorbed molecules, has not been investigated so far. In this letter, we report on quantitative measurements and modeling of conductivity and the work function changes of Si-face few layer graphene (FLG) and C-face multi-layer graphene (MLG) grown on 6H-SiC sub-

strate due to molecular adsorption of electron accepting NO_2 and electron donating NH_3 .¹⁷

Graphene samples used in this study were grown epitaxially on CMP polished Si and C-faces of semi-insulating on-axis 6H-SiC substrates by annealing them at temperatures ranging from 1300 to $1600\text{ }^\circ\text{C}$ for 1 h under high vacuum ($<10^{-5}$ Torr) in a cold-wall resistively heated SiC sublimation reactor. Details of the growth process are described elsewhere.¹⁰ For electrical and SWF measurements, ohmic contacts on graphene samples were established by indium metal press contacts, which were found to work quite well.

In order to investigate the modulation of electronic properties of epitaxial graphene films due to molecular adsorption, we utilized amperometric and potentiometric measurement techniques, which are described in detail elsewhere.^{18,19} The former provides information on the conductance changes and

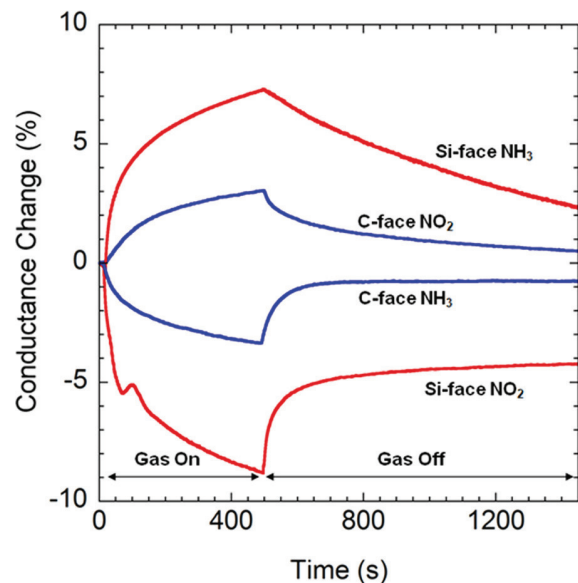


FIG. 1. (Color online) Percentage conductance changes of Si-face FLG and C-face MLG with the flow of 4 ppm NO_2 and 100 ppm NH_3 .

^{a)}Author to whom correspondence should be addressed. Electronic mail: khannoma@email.sc.edu.

the later on relative movement of the Fermi level in these films. Figure 1 illustrates the amperometric measurement results for an electron accepting (acting as a p-type dopant) gas NO_2 (4 ppm diluted in N_2) and an electron donating (acting as an n-type dopant) gas NH_3 (100 ppm diluted in N_2) flown at a rate of 30 sccm. The NO_2 adsorption causes the conductance to decrease by 9% for Si-face FLG, but increases it by 3.25% for C-face MLG in 480 s. In contrast, NH_3 adsorption increased the conductance of the Si-face FLG by 8.25% and decreases that of C-face MLG by 3.5% in 480 s. Since p-type doping by NO_2 decreases the conductivity of Si-face graphene layer and increases the conductivity of that on C-face, we infer that in the former n-type carriers are dominant, while in the later p-type charge carriers are dominant. This conclusion is also supported by the results of NH_3 adsorption, which acting as a n-type dopant, increases the conductivity of the Si-face while reducing that of the C-face. Using variable-field Hall and resistivity measurements, Lin *et al.*²⁰ reported that in thin epitaxial graphene (FLG), the carrier is n-type regardless of the face, while in MLG grown on C-face SiC, the carrier is p-type in the uppermost layers, which essentially supports our observation.

To investigate the correlation between conductance and Fermi level changes ($\Delta\sigma$ and $\Delta\phi$) in graphene films, potentiometric measurements were also performed. Results of SWF changes due to adsorption of NO_2 (4 ppm) and NH_3 (100 ppm) molecules are shown in Figs. 2(a) and 2(b). We

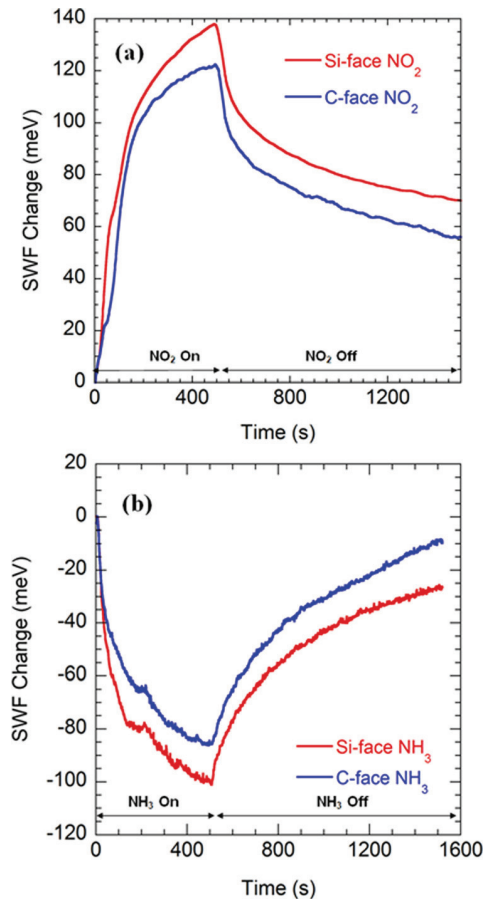


FIG. 2. (Color online) Surface work function changes of Si-face FLG and C-face MLG with the flow of (a) 4 ppm NO_2 and (b) 100 ppm NH_3 .

find that the adsorption of NO_2 causes SWF of graphene layers on Si and C-faces to increase by ~ 140 meV and ~ 120 meV, respectively within 480 s. On the other hand, for the same time interval, NH_3 adsorption causes a decrease in SWF by ~ 100 meV and ~ 85 meV for the Si and C-faces, respectively. Clearly, NO_2 adsorption implies a downward movement of the Fermi level in graphene on both Si and C-faces, while adsorption of NH_3 indicates an upward movement in the faces of graphene. These observations support the conductivity variations due to adsorption of two gases discussed above, which can be easily understood by considering the band diagram of graphene. Figures 3(a) and 3(b) show the movement of the Fermi level for both Si and C-face graphene due to adsorption of NO_2 and NH_3 molecules. As seen from Fig. 3(a), a decrease in the Fermi level of Si-face FLG, E_{F-Si} , causes a reduction in its n-type carrier density, which reduces the film conductance. On the other hand, a decrease in Fermi level of C-face MLG, E_{F-C} , [Fig. 3(b)] causes its p-type carrier density to increase, thereby increasing the film conductance. Thus, even though the SWF increases for both Si and C-faces, the conductivity decreases for the former, and increases for the later. The effect of NH_3 adsorption is also explained similarly from Figs. 3(a) and 3(b), where SWF decreases for both the faces, but conductivity changes are in opposite directions.

The Fermi level change $\Delta E_F [= (E_{F1} - E_{F0})]$, where E_{F0} and E_{F1} are the initial and final Fermi levels, respectively, and the adsorption induced changes in the charge carrier density in graphene, Δn_{ads} , are related by the equation²¹

$$\Delta n_{ads} = |(E_{F1}^2 - E_{F0}^2)| / \pi (\hbar v_F)^2. \quad (1)$$

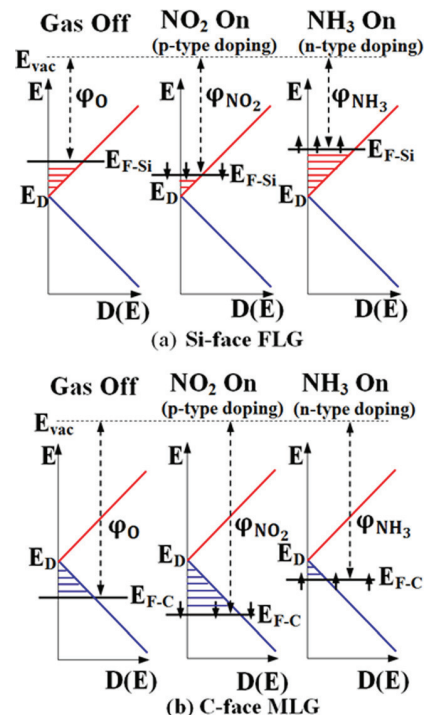


FIG. 3. (Color online) Band diagram showing decrease or increase of carrier concentration in (a) Si-face FLG and (b) C-face MLG as a result of Fermi level shift due to NO_2 or NH_3 adsorption.

Here, v_F is the Fermi velocity of electrons in the graphene film ($=10^8$ cm/s),²² and E_{F0} is the equilibrium Fermi level shifted with respect to the Dirac point, due to the presence of impurities on the film. For a typical carrier concentration²³ (also obtained from Hall measurements) $n_0 = 1 \times 10^{13}$ cm⁻² in these samples, E_{F0} calculated from the relation $n_0 = E_{F0}^2 / \pi(\hbar v_F)^2$ is 368.8 meV. Using this value of E_{F0} in Eq. (1), and using the maximum increase in SWF $\Delta\phi_{\max}$ (decrease in graphene Fermi level) due to NO₂ adsorption of 138 meV, from Fig. 2(a), we obtain $\Delta n_{\text{NO}_2} = 6.15 \times 10^{12}$ cm⁻². This would produce $\sim 60\%$ change in conductance, which is much greater than the change of $\sim 10\%$ (Fig. 1) typically measured. Same holds for NH₃ adsorption as well. Based on the relationship between NO₂ concentration and carrier density change reported by Novoselov *et al.*,⁶ for ~ 4 ppm NO₂ we should have $\Delta n_{\text{NO}_2, \max} \approx 2.5 \times 10^{11}$ cm⁻². From Eq. (1), this would result in a Fermi level change (due to charge transfer) of ~ 7 meV, which is only a few percent of the overall change of 138 meV measured experimentally. Clearly, only a small fraction ($7/138 = 5.07\%$) of the adsorbed molecules contributing to the change in SWF is actually participating in charge transfer or carrier density change. Nevertheless, assuming that the same fraction of the total SWF change at each instant is contributing to the carrier density change, we can model the change in carrier density as a function of time, $\Delta n(t)$, from the work function change transient. In the Boltzmann's transport model, the conductance G , for Fermi level away from the Dirac point, is proportional to n_0/n_{imp} .²² Thus, assuming a value of n_{imp} , we can simulate our experimentally observed conductance transient $\Delta G(t)$ from the SWF transient $\Delta\phi(t)$ using the equation,

$$\frac{\Delta G(t)}{G(t)} = \left[\left(n_0 - \Delta n(t) \right) / \left(n_{\text{imp}} + \Delta n(t) \right) - n_0 / n_{\text{imp}} \right] / \left(n_0 / n_{\text{imp}} \right). \quad (2)$$

Here, $\Delta n(t)$ is calculated from Eq. (1) at each instant, with $E_{F1}(t) = E_{F0} - 0.0507 \Delta\phi(t)$ for NO₂ adsorption. We used $n_0 = 10^{13}$ cm⁻², $\Delta n_{\text{NO}_2, \max} = 2.7 \times 10^{11}$ cm⁻², $\Delta n_{\text{NH}_3, \max} = 2.1 \times 10^{11}$ cm⁻², and $n_{\text{imp}} = 4 \times 10^{12}$ cm⁻² for both NO₂ and NH₃. Since $\Delta n_{\text{NH}_3, \max}$ for NH₃ is not known a priori, we fitted the conductance transient for NO₂ first, and then used the same n_{imp} to simulate the NH₃ transient by using $\Delta n_{\text{NH}_3, \max}$ as the fitting parameter. Please note that the signs for Δn and $\Delta\phi$ are opposite for NH₃ adsorption. The simulated and experimental conductance transients for NO₂ and NH₃ are shown together in Fig. 4, which can be seen to match quite well.

As mentioned earlier, our experimental results indicate that only a small fraction of the SWF change owing to NO₂ adsorption is caused by the movement of the Fermi level due to charge transfer. The adsorbed molecules can also contribute to electron affinity change $\Delta\chi$ due to their dipole moments, which can be written as²⁴

$$\Delta\chi = \frac{q}{\epsilon_s \epsilon_0} \theta \mu_{\text{chem}} n_{\text{chem}}, \quad (3)$$

where μ_{chem} and n_{chem} are the dipole moment and adsorption density of the molecules, and $\epsilon_s (= \epsilon_r / \sqrt{2})$ (Ref. 24) is the sur-

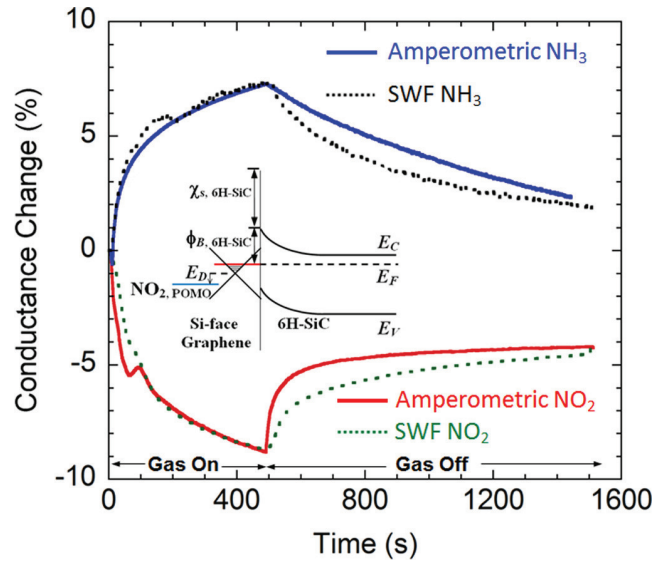


FIG. 4. (Color online) Experimentally measured conductivity transients for Si-face epitaxial graphene compared to theoretically modeled ones for NH₃ and NO₂ adsorption and desorption periods. Inset shows the Si-face graphene/6H-SiC interfacial band diagram along with the energy level of the partially occupied molecular orbitals (POMO) of the adsorbed NO₂ molecules below the Dirac point E_D .

face dielectric constant. If each NO₂ molecule accepts 0.1–0.19 e from the graphene layer,^{17,25} the molecular density of NO₂ producing $\Delta n_{\text{NO}_2, \max} = 2.7 \times 10^{11}$ cm⁻² has an upper limit of 2.7×10^{12} cm⁻². Plugging this in Eq. (3) and considering maximal coverage ($\theta = 1$) yield $\Delta\chi = \sim 2.6$ meV, assuming $\epsilon_r = 2$ for graphene, and $\mu_{\text{chem}} = 0.36$ D for NO₂. Clearly, the electron affinity change cannot account for the large change in work function observed. Another possibility is that a large fraction of the NO₂ molecules are physisorbed on the surface, i.e., they do not contribute to charge interaction but only contribute to electron affinity changes (Volkenstein Model).²⁴ Although this is possible for NH₃ due to its lower adsorption energy (which allows it to adsorb in both charge interacting and non-interacting configurations),¹⁷ it is unlikely to be the case for NO₂ due to its much larger adsorption energy of 0.3–0.4 eV,^{17,26} which forces it to accept electrons in any adsorption configuration.¹⁷ A plausible explanation of the large change in work function can be based on the charge interaction between NO₂ molecules and the graphene/SiC interfacial layer, in addition to their interaction with the graphene layer. It has been proposed that epitaxial graphene layer on Si-face SiC accept electrons from the interfacial layer (present between the SiC substrate and the graphene layer) to generate the high background carrier density n_0 .^{23,27} Since the unoccupied molecular orbitals of NO₂ are formed below the Dirac point of graphene,²⁶ it is logical to conclude that they would accept electrons from both graphene layer and the interfacial layer on the SiC substrate (see inset of Fig. 4). The later can result in a larger magnitude of transferred charge separated by a much longer distance [~ 1 nm as opposed to the dipole length of NO₂ (< 0.1 nm)], which can produce much higher change in electron affinity (and hence work function) compared to the simple molecular dipole moment considerations in Eq. (3).

In conclusion, charge carrier transport properties and molecular doping in epitaxial graphene grown on both Si and C-faces of 6H-SiC have been investigated and modeled. Our results indicate that in C-face MLG, p-type charge carriers are dominant, while in Si-face FLG, charge carriers are mostly n-type. An analytical model correlating change in conductivity with molecular doping, impurity density, and work function change has been developed utilizing Boltzmann transport theory. Our results further indicate that for epitaxial graphene grown on SiC, charging of the adsorbed molecules and related work function changes can be strongly influenced by the substrate.

Financial supports for this work from National Science Foundation (Grant Nos. ECCS-0801435, ECCS-0846898, and ECCS-1029346), Army Research Office (Grant No. W911NF-08-0299), and Structured Materials Industries, Inc. (through NSF Grant No. IIP-0930419) are thankfully acknowledged.

- ¹A. K. Geim and K. S. Novoselov, *Nature Mater.* **6**, 183 (2007).
- ²I. W. Frank, D. M. Tanenbaum, A. M. Van der Zande, and P. L. McEuen, *J. Vac. Sci. Technol. B* **25**, 2558 (2007).
- ³A. A. Balandin, S. Ghosh, W. Z. Bao, I. Calizo, D. Teweldebrhan, F. Miao, and C. N. Lau, *Nano Lett.* **8**, 902 (2008).
- ⁴K. I. Bolotin, K. J. Sikes, J. Hone, H. L. Stormer, and P. Kim, *Phys. Rev. Lett.* **101**, 096802 (2008).
- ⁵E. H. Hwang, S. Adam, and S. D. Sarma, *Phys. Rev. Lett.* **98**, 186806 (2007).
- ⁶F. Schedin, A. K. Geim, S. V. Morozov, E. W. Hill, P. Blake, M. I. Katsnelson, and K. S. Novoselov, *Nature Mater.* **6**, 652 (2007).
- ⁷J. T. Robinson, F. K. Perkins, E. S. Snow, Z. Wei, and P. E. Sheehan, *Nano Lett.* **8**, 3137 (2008).
- ⁸M. Foxe, G. Lopez, I. Childres, R. Jalilian, C. Roecker, J. Boguski, I. Jovanovic, and Y. P. Chen, IEEE Nuclear Science Symposium Conference, Orlando, FL, USA, October 25-31, 2009.
- ⁹K. V. Emtsev, A. Bostwick, K. Horn, J. Jobst, G. L. Kellogg, L. Ley, J. L. McChesney, T. Ohta, S. A. Reshanov, J. Röhl *et al.*, *Nature Mater.* **8**, 203 (2009).
- ¹⁰S. Shivaraman, M. V. S. Chandrashekar, J. Boeckl, and M. G. Spencer, *J. Electron. Mater.* **38**, 725 (2009).
- ¹¹S. Shivaraman, R. A. Barton, X. Yu, J. Alden, L. Herman, M. V. S. Chandrashekar, J. Park, P. L. McEuen, J. M. Parpia, H. G. Craighead *et al.*, *Nano Lett.* **9**, 3100 (2009).
- ¹²Md. W. K. Nomani, R. Shishir, M. Qazi, D. Diwan, V. B. Shields, M. G. Spencer, G. S. Tompa, N. M. Sbrockey, and G. Koley, *Sens. Actuators B* **150**, 301 (2010).
- ¹³Y. Shi, K. K. Kim, A. Reina, M. Hofmann, L. J. Li, and J. Kong, *ACS Nano* **4**, 2689 (2010).
- ¹⁴Y. J. Yu, Y. Zhao, S. Ryu, L. E. Brus, K. S. Kim, and P. Kim, *Nano Lett.* **9**, 3430 (2009).
- ¹⁵N. J. Lee, J. W. Yoo, Y. J. Choi, C. J. Kang, D. Y. Jeon, D. C. Kim, S. Seo, and H. J. Chung, *Appl. Phys. Lett.* **95**, 222107 (2009).
- ¹⁶M. Qazi, Md. W. K. Nomani, M. V. S. Chandrashekar, G. Koley, V. B. Shields, and M. G. Spencer, *Appl. Phys. Exp.* **3**, 075101 (2010).
- ¹⁷O. Leenaerts, B. Partoens, and F. M. Peeters, *Phys. Rev. B* **77**, 125416 (2008).
- ¹⁸G. Koley, M. Qazi, L. Lakshmanan, and T. Thundat, *Appl. Phys. Lett.* **90**, 173105 (2007).
- ¹⁹M. Qazi, T. Vogt, and G. Koley, *Appl. Phys. Lett.* **91**, 233101 (2007).
- ²⁰Y. Lin, C. Dimitrakopoulos, D. B. Farmer, S. Han, Y. Wu, W. Zhu, D. K. Gaskill, J. L. Tedesco, R. L. Myers-Ward, C. R. Eddy, Jr., *et al.*, *Appl. Phys. Lett.* **97**, 112107 (2010).
- ²¹Z. Chen, I. Santoso, R. Wang, L. F. Xie, H. Y. Mao, H. Huang, Y. Z. Wang, X. Y. Gao, Z. K. Chen, D. Ma *et al.*, *Appl. Phys. Lett.* **96**, 213104 (2010).
- ²²S. Adam, E. H. Hwang, V. M. Galitski, and S. D. Sarma, *Proc. Natl. Acad. Sci. U.S.A.* **104**, 18392 (2007).
- ²³C. Riedl, C. Coletti, and U. Starke, *J. Phys. D: Appl. Phys.* **43**, 374009 (2010).
- ²⁴H. Geistlinger, I. Eisele, B. Flietner, and R. Winterb, *Sens. Actuators B* **34**, 499 (1996).
- ²⁵Y. H. Zhang, Y. B. Chen, K. G. Zhou, C. H. Liu, J. Zeng, H. L. Zhang, and Y. Peng, *Nanotechnology* **20**, 185504 (2009).
- ²⁶T. O. Wehling, K. S. Novoselov, S. V. Morozov, E. E. Vdovin, M. I. Katsnelson, A. K. Geim, and A. I. Lichtenstein, *Nano Lett.* **8**, 173 (2008).
- ²⁷W. Chen, S. Chen, Z. Hua Ni, H. Huang, D. Chen Qi, X. Yu Gao, Z. Xiang Shen, and A. Thyé Shen Wee, *Jpn. J. Appl. Phys.* **49**, 01AH05 (2010).